Nonadiabatic phenomena during magnetic trap confinement and their influence on maximum x-ray energy from electron-cyclotron-resonance-heated plasmas

K. S. Serebrennikov,* C. Gaudin, J.-M. Buzzi, J. Bruneteau, and C. Rouille
Laboratoire de Physique des Milieux Ionisés, UMR 7643 du CNRS, Ecole Polytechnique, 91128 Palaiseau, France
(Received 29 July 1998; revised manuscript received 6 December 1999; published 26 March 2001)

Nonadiabatic effects during the confinement of energetic electrons with a gyroradius comparable with the magnetic field scale have been studied with a phase section technique. The appearance of a hot electron component is a characteristic feature of electron-cyclotron-resonance-heated plasma production in magnetic mirrors. A criterion for the absence of stable trajectories and the transition to strong stochastic motion for any initial condition is proposed and confirmed by simulations. Satisfactory agreement with the experimental x-ray spectra is obtained.

DOI: 10.1103/PhysRevE.63.046405 PACS number(s): 52.55.Dy, 52.20.Dq, 52.50.Gj, 52.70.La

I. INTRODUCTION

Numerous experiments on the heating of plasmas by microwave sources based on electron-cyclotron resonance [1–6] have proved the efficiency of this method for generating plasmas with densities up to $10^{12}-10^{14}\,\mathrm{cm}^{-3}$. If the plasma is confined in a trap by a mirror magnetic field, a hot electron ring appears in the central plane of the trap [2]. This ring is localized in the zone of resonance between the microwave frequency ω and the cyclotron frequency ($\omega=\omega_c$), or with any harmonics of the cyclotron frequency ($\omega=n\omega_c$).

The width of the ring is relatively small, so for longitudinal and transverse components of electron momentum with respect to the magnetic field, the inequality $p_\parallel/p_\perp \ll 1$ holds. This relation shows that, during the heating, it is the transverse component that is mainly increased. The maximum energy in the electron power spectrum during the confinement in a relatively high magnetic field (several kG) can approach 1 MeV. Such energies are observed even at low microwave power (<1 kW) [3].

Early experiments in the years 1960–1990 were designed to create a thermonuclear plasma with magnetic mirrors. However, it was recently demonstrated that the formation of hot electron annular rings is also possible on compact devices with intermediate and weak magnetic fields (<1 kG) and low microwave power [7]. Such devices can be used for the generation of x rays [8], and other purposes [9].

For a time duration of several bounce oscillations, the influence of the rf electric field E on the motion of an energetic electron ($W>10\,\mathrm{keV}$) in a magnetic field remains weak because the parameter $g=E/(cB)$ is small. For a low density plasma ($n\sim10^{11}-10^{12}\,\mathrm{cm}^{-3}$), when the frequency of Coulomb collisions is considerably less than the cyclotron frequency, the confinement of an energetic electron in intermediate and weak magnetic fields is determined by nonadiabatic effects [10]. Numerical simulations of electron trajectories, in the strong magnetic fields of the Bumpy Torus experiments [11,12], also confirm this statement. Under these conditions it is possible to assume that the role of heating is reduced to a slow increase of the energy of the electron, and the maximum energy at which the electron must leave the trap is determined by the confinement.

The aim of this research was to study the maximum energy of the electrons determined by the confinement without entering into a detailed description of the electron heating mechanism. Of course, this mechanism should exist to generate hot electrons, but we suggest that it should not change the criterion of confinement of high-energy electrons.

We shall study the confinement of energetic electrons, whose gyroradii are comparable with the magnetic field scale, relying on a phase section technique. To be more specific the calculations will be carried out with the magnetic field of a real device [13], and numerical results will be compared with experimental ones.

II. PHASE PLANE SECTIONS

Rather deep insight into the problem of chaotic motion can be obtained with the help of a technique similar to Poincaré cross sections (see, for example, Ref. [14]), which is a customary tool for studying nonintegrable systems such as the equations of particle motion in an inhomogeneous magnetic field.

We perform the simulations of particle trajectories in the magnetic mirror created by two permanent magnets with a field strength on their surfaces of about 4.5 kG. The distance between the magnets yields the field intensity in the center of the trap. The motion of an electron is calculated, in the single particle approximation, with the use of relativistic equations in a nonuniform magnetic field. For phase section calculations, the particle energy change is neglected, as we consider a time interval much smaller than the characteristic time of energy gain from the rf external field.

Here we shall give the reasons for our choice of phase variables. Let us introduce a cylindrical frame of reference (r, ψ, z), whose center coincides with the center of the magnetic trap, the direction of the z axis being the direction of the magnetic force line on the axis of symmetry. The Hamiltonian describing the electron motion as a function of

*Permanent address: Russian Research Center ''Kurchatov Institute,'' Russia.

canonical momenta and coordinates does not depend either on the time or on the angle ψ of the cylindrical coordinates, since the vector potential for the axisymmetric magnetic field $A_\psi(r,z)$ depends on r and z only:

$$H=c\left[m_0^2c^2+P_r^2+P_z^2+\left(\frac{P_\psi}{r}+eA_\psi(r,Z)\right)^2\right]^{1/2}, \quad (1)$$

where m_0 is the electron rest mass, c is the velocity of light, and e is the absolute value of electron charge. Thus we have two invariants: the conservation in time of both the kinetic electron energy W; and the momentum conjugate to ψ, i.e., P_ψ,

$$P_\psi=rp_\psi-erA_\psi(r,z)=\text{const}, \quad (2)$$

where $p_\psi=mr(d\psi/dt)$, $m=\gamma m_0$, and γ is the relativistic Lorentz factor.

The existence of two integrals of motion permits one to reduce the system of canonical equations from sixth order to a system of fourth order. The latter has the form of equations that describe the oscillations of a particle in a two-dimensional potential well,

$$\frac{dp_r}{dt}=-\frac{\partial}{\partial r}u(r,z), \quad \frac{dr}{dt}=\frac{p_r}{m},$$

$$\frac{dp_z}{dt}=-\frac{\partial}{\partial z}u(r,z), \quad \frac{dz}{dt}=\frac{p_z}{m},$$

with an effective potential

$$u(r,z)=\frac{[P_\psi+erA_\psi(r,z)]^2}{2mr^2}. \quad (3)$$

Depending on the sign of the constant of motion P_ψ, different physical situations can occur. If $P_\psi<0$, then the minimum of the effective potential is equal to zero for all z. The position of the minimum is found from the equation $P_\psi=-erA_\psi(r,z)$, which is also the equation of constant magnetic flux. This means that an electron during the oscillations near the minimum of the potential well [Eq. (3)] actually rotates around the magnetic lines on the same magnetic surface. In principle, it can leave the trap by moving in the longitudinal direction. According to Eq. (2), the sign of the angular momentum p_ψ is changed as it passes through the minimum of the effective potential. In the real three-dimensional space, this means that the electron trajectory does not enclose the z axis during one single cyclotron rotation. In the case where $P_\psi>0$, the value of the minimum of the effective potential is increased at the approach to mirror throats; therefore, an electron is better confined in the longitudinal direction. The rest of this paper concerns only the case $P_\psi<0$, which corresponds to the following experimentally observable picture.

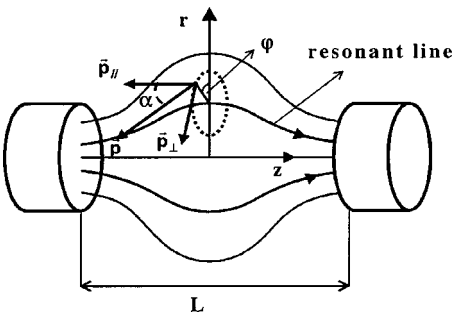

FIG. 1. Illustration of the choice of phase coordinates.

(1) Formation of the hot electron ring takes place near the midplane of the trap around the resonant magnetic line. The radius of this line is obtained from the resonance condition

$$\frac{eB(R_{\text{res}})}{m}=\omega_{\text{res}}, \quad (4)$$

where ω_{res} is the microwave frequency, and $B(r)$ is the absolute value of the magnetic field as a function of the radius in the midplane. (Here it is implied that the heating is done at the fundamental harmonic cyclotron frequency, meeting the experimental conditions described in Sec. V. However, the conclusions obtained below can also be applied for heating at other multiple harmonics.)

(2) The radius of the resonant line in the midplane is larger than the gyroradius of the hottest electrons in the ring. (This condition will be satisfied for magnetic configurations used for calculations of phase sections, and for the experimental recording of spectra described in Sec. V.)

From a mathematical point of view, if one fixes a particular magnetic line [in our case from Eq. (4)] and chooses $z=0$ (midplane), then there remain three free parameters (including the energy). Their choice completely characterizes the electron trajectory. Following Refs. [10,14], as the other two parameters we shall choose: (a) the sine of the absolute value of the pitch angle α, which is unequivocally connected to the magnetic moment of the electron; and (b) the gyrophase φ (see Fig. 1).

The electron trajectory in the midplane (if the electron has only a transverse momentum $p_\perp$) is conventionally represented as a Larmor circle (dashed line). In reality, especially in the case of large gyroradii, this trajectory has a more complex form due to the inhomogeneity of the magnetic field, which causes the instantaneous value of the gyroradius to depend on the position. Nevertheless, we can define the gyrophase as the angle between the radius vector passing through the instantaneous center of the gyrorotation and the vector going from this gyrocenter to the given point of the trajectory. The gyrophase is increased in the direction of electron rotation. This definition relates the gyrophase to the position of the electron on the trajectory. The trajectory itself, at a given value of transverse momentum in the midplane, can be unequivocally fixed with respect to the chosen resonant line, since from Eq. (2) the point on the trajectory where $p_\psi=0(|p_r|=p_\perp)$ should have a radius equal to the radius of a resonant line R_{res}.

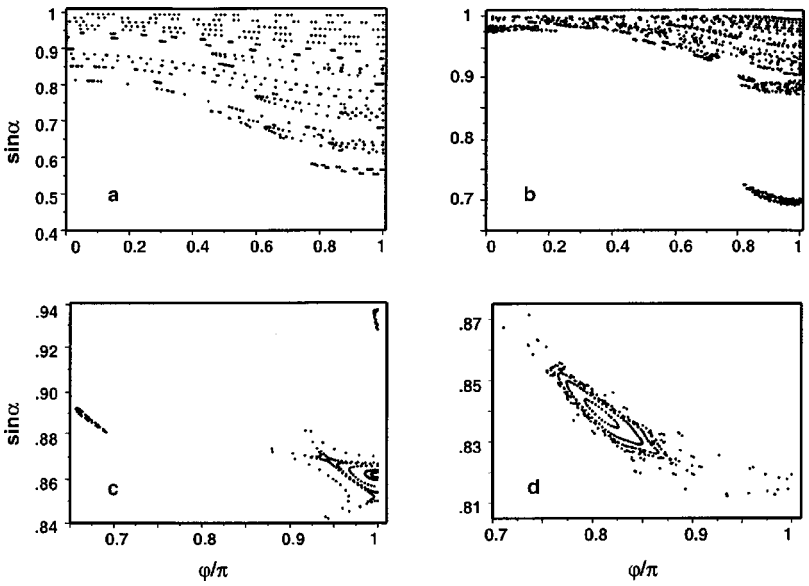

FIG. 2. Phase plane section taken at the midplane. The parameters of trajectories (α pitch angle; φ gyrophase) are chosen at successive crossings of the midplane. (a) $W=5$ keV. (b) $W=20$ keV. (c) $W=30$ keV. (d) $W=35$ keV. (Only the half-part is shown as the plots are symmetrical with respect to $\varphi=0$.) The magnetic field configuration corresponds to 6.2 cm between the magnets.

The plane of the chosen phase coordinates, at the given energy of the electron and a fixed magnetic line, represents the phase section of a four-dimensional phase volume. The method of phase section calculation consists of setting different initial parameters for the electron in the midplane (pitch angle and gyrophase), and then registering them at the subsequent intersections of this midplane by the trajectory. Each intersection corresponds to a point in the plane [φ, $\sin(\alpha)$].

The plots for four different energies of the electron (W), in the case of a distance of 6.2 cm between the magnets defining the mirror, are presented in Fig. 2. The set of crossing points corresponding to the electron trajectory form of the phase portrait (phase trace) of this trajectory. From its behavior, one can draw conclusions about the stability of a trajectory. For a stable (or regular) trajectory, points of crossing either lie on a closed line or form a periodic set in φ. Otherwise, the phase portrait reveals a limited set of chaotically located points. Electrons on such an unstable trajectory undergo some bounce oscillations, and then leave the trap through the throats.

In Fig. 2 only regions of regular trajectories (stable regions) are shown, as these regions occupy only a small part of the whole plane, and the blank areas correspond to chaotic trajectories. In Figs. 2(c) and 2(d) an adjacent area of weak stochasticity has been added to the graphs (nonclosed lines), in order to emphasize better the structure of the stable regions.

Phase section plots clearly show that severe restrictions are imposed by nonadiabaticity on the behavior of energetic electrons. According to adiabatic theory, the phase trace should to be a straight line $\sin(\alpha)=$const, and the stable region should occupy all the area outside the loss-cone $\sin(\alpha)>0.44$ (this inequality corresponds to a mirror ratio along the resonance line of about 5). However, even at an electron energy of $W=5$ keV [Fig. 2(a)], the region where the regular motion is possible is much less than the one predicted by adiabatic theory. In addition, the magnetic moment of the electron [$\mu\sim\sin^2(\alpha)$] is changed from one intersection of the midplane to another. For more energetic particles, the stable regions shrink [Figs. 2(b)–2(d)], and finally for $W=40$ keV we could not find any initial conditions in the midplane for the trajectory to be stable. Thus there exists a maximum energy which is determined by the magnetic field structure.

These nonadiabatic restrictions may also play a significant role in determining the electron energy distribution function of the hot electron component during plasma heating. The boundary conditions for the Fokker-Planck equation, which follow from the complex form of stable regions on the phase plane, can strongly influence parameters of the distribution function such as the temperature [11].

It is interesting to observe that when approaching the maximum energy, the stable regions of the phase space for energetic particles become small enough [Figs. 2(c) and 2(d)] that corresponding regular trajectories have a definite form. For example, Fig. 3 shows the trajectory corresponding to the stable region in Fig. 2(d). In Fig. 3, we can also easily see that the form of the trajectory corresponds to the first resonance between gyrorotation and bounce oscillations of the electron (see Sec. IV). The characteristic feature of this particular trajectory is that it is not symmetric with respect to the midplane.

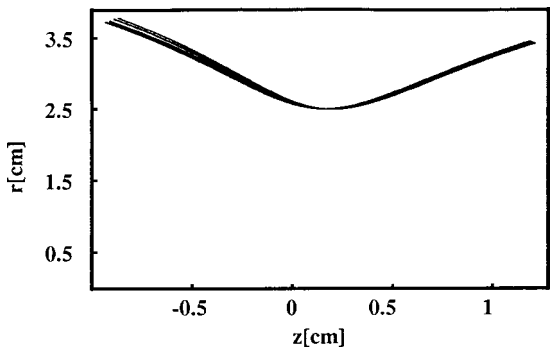

FIG. 3. Stable trajectory corresponding to the regular area of Fig. 1(d).

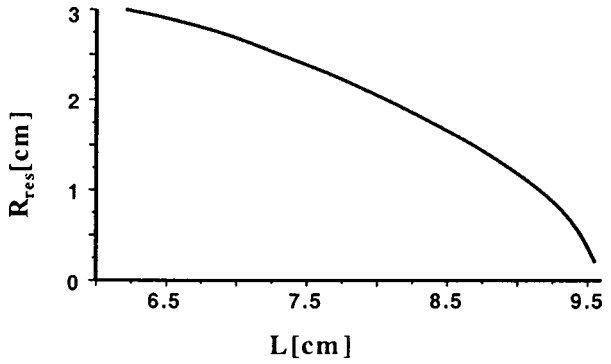

FIG. 4. Radius of the resonance line in the midplane of the trap as a function of the distance between the magnets, L.

III. ANOTHER APPROACH TO DETERMINE THE MAXIMUM ENERGY

The construction of phase sections gives information about the form of stable areas and about the maximum attainable energy. However, if it is necessary to determine the maximum energy for a large number of magnetic configurations (for the purpose of looking at an optimum magnetic configuration for some applied problem), it is possible to offer another method less demanding of computer time than the method of phase sections. This method consists of modeling the heating by a slow increase of the electron energy with time; that is, slow with respect to the period of bounce oscillations. The additional term is added to the equation of motion, and it should be such that it does not cause a premature departure of the particle from the trap.

For subsequent calculations, we have chosen the ''heating'' term in the following form:

$$\frac{dp_\perp}{dt} = \frac{g}{[1+(z^2/\Lambda^2)]}. \tag{5}$$

Here z is the coordinate along the axis of the magnetic field, measured from the central plane, Λ is the longitudinal characteristic dimension of resonant area, $g \sim E/(cB_{\rm res}) \ll 1$, $p_\perp$ is the transverse electron momentum normalized to mc, and t is the time normalized to the inverse cyclotron frequency.

The electron is located originally on a resonant line, with a small energy close to the energy of ionization. In the absence of collisions, the electron trajectory is modified slowly with time, so that its phase trace always lies in the stable region (see Fig. 2), even when the latter becomes very small. Finally, when reaching a certain energy, the stable region disappears, as indicated in Sec. II, and the particle leaves the trap after a few chaotic oscillations. This energy is thus the maximum energy the electron can have in such a magnetic configuration.

We have carried out four simulations for various magnetic field configurations, corresponding to distances between the magnets (L) of 6.2, 7.2, 8.6, and 9 cm. To explain the difference between these configurations, Fig. 4 shows the dependence of the radius of the resonant lines in the midplane, $R_{\rm res}$, versus L for the working frequency $\omega_{\rm res} = 2\pi\, 2.45$ GHz. In all cases, the electron rotates along a Larmor circle that does not enclose the axis of symmetry of the field.

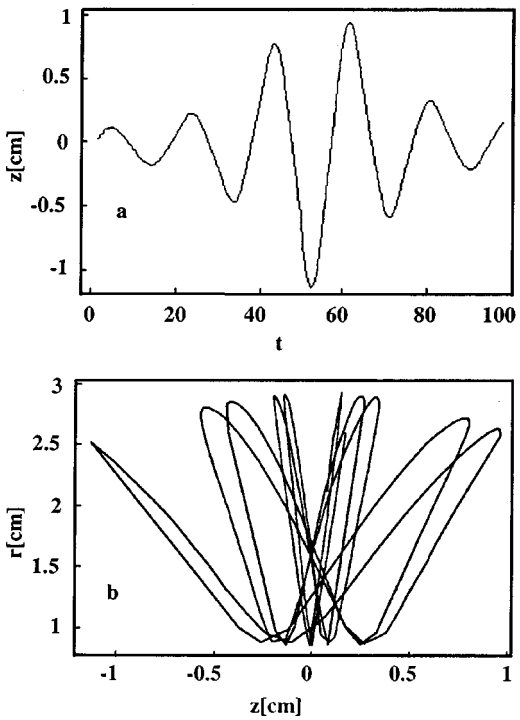

FIG. 5. End point oscillations (a) and electron trajectory for the same time interval (b). $L = 8.6$ cm and $W = 66$ keV. t is the time normalized to ω^{-1}.

The slow energy change in time permits one to follow the dynamics of a regular electronic trajectory. The characteristic features of the electron behavior are oscillations of the magnetic moment, which are manifested by oscillations of the reflection points at the mirror ends [see Fig. 5(a); in Fig. 5(b) the electron trajectory is shown in the plane (r, z) for the same time duration]. The amplitude of these oscillations increases with energy, in accordance with Ref. [14]. Near the maximum energy, the magnetic moment oscillations become irregular. This is illustrated in Fig. 6, where the time dependence of the electron longitudinal coordinate is shown just

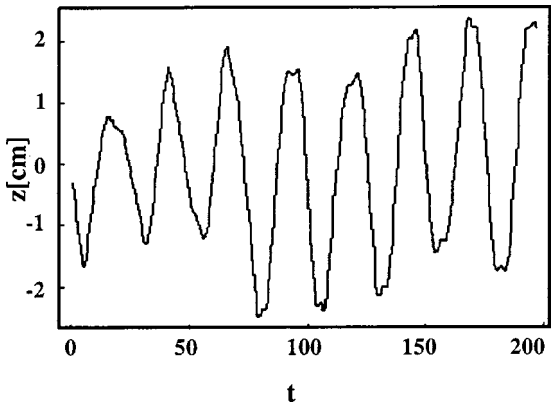

FIG. 6. End point oscillations in the chaotic region. $L = 8.6$ cm and $W \approx 70$ keV. t is the time normalized to ω^{-1}.

TABLE I. Calculated values of maximum energy W_{max} along with the characteristic parameter of the resonant magnetic line and its relation to the gyroradius.

Distance between magnets L (cm)	Maximum energy W_{max} (keV)	Line parameter l (cm)	ρ/l[a]
6.2	38	1.75	0.44
7.2	52	2.06	0.44
8.6	70	2.56	0.41
9	90	2.73	0.44

[a]Here ρ is taken at an energy equal to W_{max}.

before leaving the trap. Figure 6 also illustrates that the electron (which is on an irregular trajectory) still has the time to make several bounce oscillations, the number of which cannot be determined precisely. As it continues to interact with an external field, the maximum observable energy in the experiment can be a slightly larger than the value determined from the condition of the disappearance of the stable region.

In all cases, during a period of several cyclotron gyrations, the phase trace of particle motion in the midplane is similar to those discovered in Sec. II with constant energy. Practically the same behavior and the same maximum energies are obtained with different values of g or Λ, even when the structure of the heating term was changed. The calculated values of the maximum energies are listed in Table I.

IV. CRITERION FOR THE ABSENCE OF REGULAR MOTION

As shown in Ref. [15], nonconservation of the magnetic moment arises from a nonlinear resonant interaction of the gyromotion with harmonics of the bounce motion. In our calculations, in all cases, the disappearance of the last stable region occurs near the first resonance between the gyrorotation and the bounce oscillation of the electron ($\overline{\omega}=2\Omega$), where $\overline{\omega}$, is an average cyclotron frequency, and Ω is the bounce frequency. The Chirikov theory presented in Ref. [10] is then not applicable in our case, as it was deduced with the assumption of higher-order resonances ($\overline{\omega}\gg 2\Omega$). The Chirikov criterion is reached when there is resonant overlapping in amplitude between two oscillators. There is a threshold for stochasticity that has been verified in numerous numerical experiments. This criterion holds when the two frequencies are distinct. In our case, we have a frequency degeneracy since $\overline{\omega}=2\Omega$, and then the Chirikov criterion can no longer be satisfied. The energy boundary for the presence of any regular motion can be described by a heuristic ratio

$$\frac{\rho}{l}\approx\frac{1}{2}, \tag{6}$$

where $\rho=|v|/\omega$ is the total gyroradius at $z=0$ and l is related to the curvature of the magnetic field line

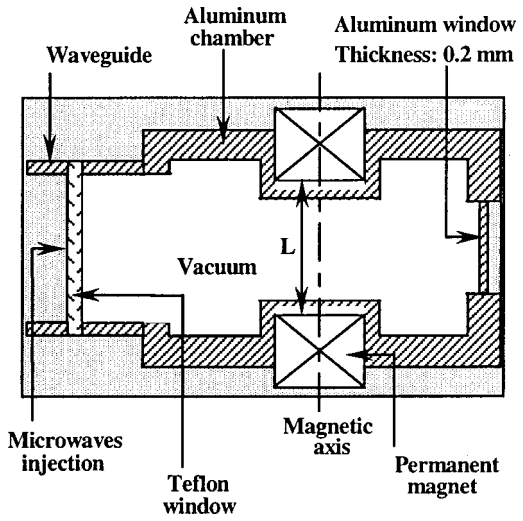

FIG. 7. Schematic description of the chamber.

$$l=\left(\frac{2B_0}{B''}\right)^{1/2}=\frac{\sqrt{2}B_{z0}}{\sqrt{2(\partial B_z/\partial r)^2+B_{z0}(\partial^2 B_z/\partial z^2)}}$$

The derivative here is taken along the magnetic line. The values of l and of the ratio ρ/l are also presented in Table I. Equation (6) expresses that the system is near the first resonance ($\omega=\omega_c$) [16].

A similar empirical relation between l and ρ_T, namely, $\rho_T/l\approx 0.05$, is known to be valid for most of electron-cyclotron-resonance machines [17], where ρ_T is the gyroradius corresponding to the temperature of the hot electron population. This ratio also indicates the onset of nonadiabatic particle motion, while Eq. (6) indicates the lack of any regular motion.

V. EXPERIMENTAL SETUP AND X-RAY SPECTRA FROM THE PLASMA

The main purpose of the experimental investigation was to study the Bremsstrahlung spectra of the hot electrons from the midplane of the mirror trap, and to compare them with the results of calculations presented in the above sections. Figure 7 schematically shows the plasma chamber. In a cylindrical aluminum cavity, two Sm-Co disk poles from the mirror trap. A steady-state argon plasma at a pressure in the range $(1-10)\times 10^{-5}$ Torr is sustained by microwave ($f=\omega/2\pi=2.45$ GHz, 400 W) input power. Details of the experimental device and preliminary results were published elsewhere [8,13].

In this experiment, we can easily change the distance between the permanent magnets, L, in order to vary the magnetic configuration in the chamber. Figure 8 presents the profiles of two resonant magnetic lines for the extreme cases of L equal to 6.2 and 9 cm, along with the plots of constant magnetic field. Between these two distances the homogeneity of the field increases continuously with the line characteristic parameter l [see Eq. (6) and Table I].

The pinhole camera x-ray image of the chamber, described in Ref. [13], allows one to detect the presence of the

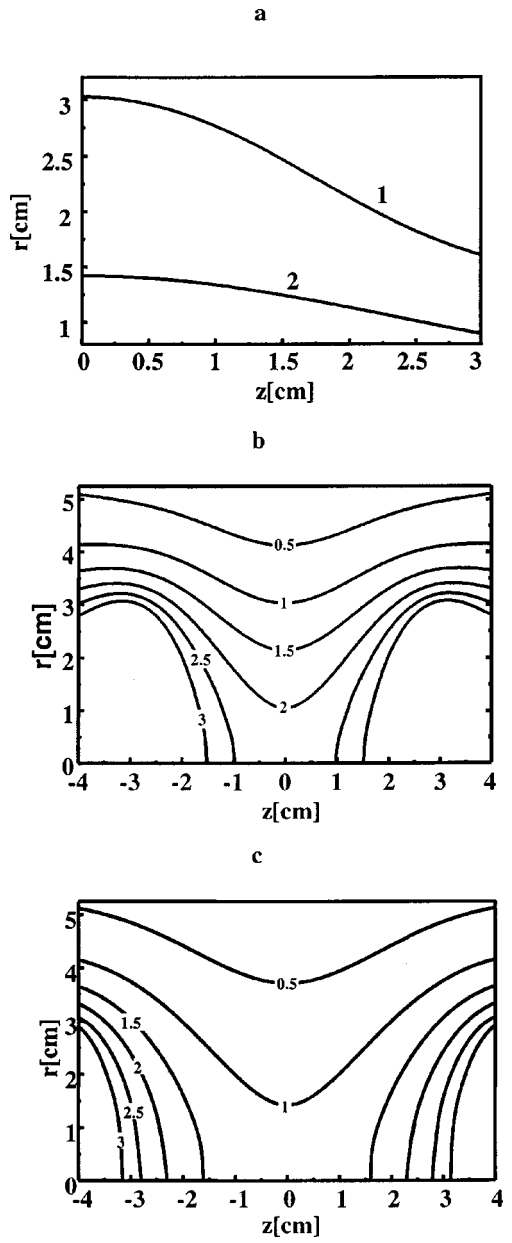

FIG. 8. (a) Profile of resonance magnetic field lines for (1) $L=6.2$ cm and (2) $L=9$ cm. Contour plots for $|B/B_{\mathrm{res}}|=\mathrm{const}$ at (b) $L=6.2$ cm and (c) $L=9$ cm.

hot electron ring near the resonant line by its images on the endplate walls of the mirror trap. No trace of x-ray emission coming from the cylindrical wall (i.e., in the radial direction) was observed. The fact that the x-ray image of the ring created by hot electrons leaving the trap also had a ringlike form proves that the electron trajectories did not enclose the magnetic field axis (see Sec. II).

Along with the generation of a hot component, the formation of a cold plasma component takes place. The latter could be observed by its optical emission in the visible. Plasma probe measurements provide an estimation of plasma density in the plasma peripheral region. We found the density to be in the range $10^{9}-10^{10}\,\mathrm{cm}^{-3}$. A relatively low plasma density indicates that the TE_{111} resonator mode was excited in the chamber.

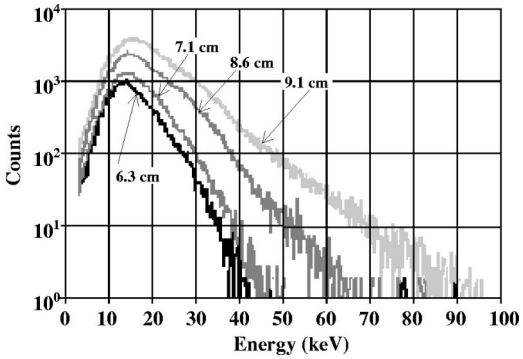

FIG. 9. X-ray spectra from the core plasma of the trap for various distances between the magnets. (a) $L=6.3$ cm. (b) $L=7.1$ cm. (c) $L=8.6$ cm. (d) $L=9.1$ cm.

We have investigated the x-ray emission in argon for different magnetic configurations corresponding to those used in the above calculations. Emission spectra were obtained in a plasma at an argon pressure of 7.5×10^{-5} Torr, and a microwave power of 400 W. We have recorded the photon spectrum with a NaI detector (1-in diameter, 2 mm thick). The 0.2-mm-thick aluminum window served to filter out the x rays with low energy. Two diaphragms made of lead with openings 2 and 5 mm in diameter were used to collimate and analyze the emission coming only from the plasma midplane. There was no detectable radiation coming from the walls. The solid angle of collimation was 4×10^{-4} st. From Bremsstrahlung analysis [18,19], we have estimated that the hot electron density in a slice of plasma around the midplane is about $10^{8}-10^{9}\,\mathrm{cm}^{-3}$.

Four such spectra are presented in Fig. 9 for distances between the magnets close to those of the calculations. The exposure time was 4 min. We suppose that an agreement exists between the maximum energy of the spectra and the calculated values from Table I, despite the background noise in the low count range. It is worth noting that the total spectral energy increases with the maximum energy, as both values depend on the mean time spent by the particle in the trap.

VI. CONCLUSION

The results presented above demonstrated that limitations on heating the plasma in the magnetic trap with a rather powerful method such as electron-cyclotron-resonance heating are not determined only by the nature of heating, but by intrinsically nonadiabatic motion in the inhomogeneous magnetic field. Our conclusion is valid at least for compact traps with intermediate values of magnetic fields (<1 kG), which are of interest now for various applications in physics and technology.

The criterion for maximum energy in the trap has been deduced for the particles following the magnetic line crossing the electron-cyclotron-resonance surface [Eq. (6)]. Satisfactory agreement between experimental and numerical results for the same conditions was demonstrated.

The use of the Poincaré sections technique revealed an interesting detail: for energies not too small with respect to

those deduced from Eq. (6), only trajectories of a definite form can be stable. The fact that the trajectories of the hot electrons are known in a given magnetic field can be used, for example, for calculating their interaction with external waves. On the other hand, these trajectories can be very useful in determining the better position of insertion of a solid target probe for the purposes of diagnostics or for x-ray production.

ACKNOWLEDGMENTS

We are grateful to Dr. M. Bacal, Professor A. A. Ivanov, and Dr. T. Lehner for constant interest and stimulating discussions. K.S.S. is grateful for financial support from Le Ministère de l'Education Nationale, de l'Enseignement Supérieur et de la Recherche, and C. G. for support from DRET (Contract No. DRET/96/1200/A00).

[1] R. A. Dandl, A. C. England, W. B. Ard, H. O. Eason, M. C. Becker, and G. M. Haas, Nucl. Fusion **4**, 344 (1964).
[2] H. Ikegami, H. Ikezi, M. Hosokawa, S. Tanaka, and K. Takayama, Phys. Rev. Lett. **19**, 778 (1967).
[3] B. H. Quon, R. A. Dandl, W. DiVergilio, G. E. Guest, L. L. Lao, N. H. Lazar, T. K. Samec, and R. F. Wuerker, Phys. Fluids **28**, 1503 (1985).
[4] S. Hiroe *et al.*, Nucl. Fusion **28**, 2249 (1988).
[5] V. A. Zhil'tsov, A. A. Skovoroda, and A. G. Shcherbakov, Fiz. Plazmy **17**, 785 (1991) [Sov. J. Plasma Phys. **17**, 456 (1991)].
[6] H. Shoyama, M. Tanaka, S. Higashi, Y. Kawai, and M. Kono, J. Phys. Soc. Jpn. **65**, 2860 (1996).
[7] K. S. Golovanivsky, V. D. Dougar-Jabon, and D. V. Reznikov, Phys. Rev. E **52**, 3 (1995).
[8] M. Bacal, C. Gaudin, A. Bourdier, J. Bruneteau, J. M. Buzzi, K. S. Golovanivsky, L. Hay, C. Rouillé, and L. Schwartz, Nature (London) **384**, 421 (1996).
[9] K. S. Golovanivsky, J. Bruneteau, M. Bacal, J. M. Buzzi, R. Geller, M. D. Karetnikov, and L. H. Schwartz, Rev. Sci. Instrum. **67**, 1267 (1996).
[10] B. V. Chirikov, Phys. Rep. **52**, 265 (1979).
[11] L. W. Owen, L. E. Deleanu, and C. L. Hedrick, in *Hot Electron Ring Physics: Proceedings of the 2nd Workshop*, edited by N. A. Uckan (Oak Ridge National Laboratory, Oak Ridge, TN, 1982), Vol. 1, p. 909.
[12] R. E. Juhala, M. A. Prelas, and C. B. Wallace, in *Hot Electron Ring Physics: Proceedings of the 2nd Workshop* (Ref. [11]), Vol. 1, p. 425.
[13] C. Gaudin, L. Hay, J. M. Buzzi, and M. Bacal, Rev. Sci. Instrum. **69**, 890 (1998).
[14] R. H. Cohen, G. Rowlands, and J. H. Foote, Phys. Fluids **21**, 627 (1978).
[15] B. V. Chirikov, Sov. J. At. Energy **6**, 630 (1959).
[16] E. M. Krushkal, Zh. Tekh. Fiz. **42**, 2288 (1972) [Sov. Phys. Tech. Phys. **17**, 1792 (1973)].
[17] N. A. Uckan, Phys. Fluids **25**, 2381 (1982).
[18] C. Gaudin, Thèse de l'Université Paul Sabatier, Toulouse, France, 1999.
[19] M. Lamoureux and N. Avdonina, Phys. Rev. E **55**, 912 (1997).